RSC Advances

ROYAL SOCIETY OF CHEMISTRY

www.rsc.org/advances

Journal Name

RSCPublishing

ARTICLE

A novel chiral electrochemiluminescence sensor that can discriminate proline enantiomers

Cite this: DOI: 10.1039/x0xx00000x

Qinghong Wang, Xia Lin, Dongmei Guo, Juanjuan Xu, Chunzhi Xuan, Cui Chen,Yingzi Fu*

Received ooth January 2012,
Accepted ooth January 2012

DOI: 10.1039/x0xx00000x

www.rsc.org/

A sensitive, stable and stereoselective electrochemiluminescence (ECL) sensor has been designed to enantioselectively discriminate proline enantiomers by immobilizing $Ru(bpy)_3^{2+}$-gold nanoparticles (Ru-AuNPs) and β-cyclodextrin-reduced graphene oxide (β-CD-rGO) on glassy carbon electrode. More $Ru(bpy)_3^{2+}$ could be immobilized on the surface of electrode stably via preparing Ru-AuNPs and better stereoselectivity could be introduced to the sensor via the synthesis of β-CD-rGO. When the developed sensor interacted with proline enantiomers, obvious difference of ECL intensities towards *L*- and *D*-proline was observed, and a larger intensity was obtained from *D*-proline. As a result, ECL technique might act as a promising method to chiral recognize of amino acids enantiomers or chiral drugs.

Introduction

Chirality is one of the most fundamental and crucial properties of various natural systems,[1] and chiral recognition plays a very important role in understanding the interactions of biological molecules. Amino acids, as the building blocks for peptides, possess chirality.[2] Furthermore, amino acids enantiomers have identical physical and chemical properties but may exhibit different physiological and biochemical behaviors in biological processes. For example, *L*-proline (*L*-Pro) is a pivotal neuronal modulator or transmitter candidate in the central nervous system,[3] while *D*-proline (*D*-Pro) is also prestent in mammals.[4] But the *D*-Pro in liver might cause periportal fibrosis and necrosis of liver cells, and severe proximal tubular dystrophy and necrosis in kidney.[5] So it is especially important to enantioselectively detect Pro enantiomers by using effective methods.

Laboratory of Luminescence and Real-Time Analysis(Southwest University), Ministry of Education, College of Chemistry and Chemical Engineering, Southwest University, Chongqing 400715, PR China PR China. Corresponding author: Fax: +86-023-68253195; Tel: +86-023-68252360; E-mail address: fyzc@swu.edu.cn.

Electrochemiluminescence (ECL), as a new developing and powerful analytical tool for detection, has been widely used to chemical and biological analysis based on its distinct advantages of simplicity, rapidity, sensitivity, controllability and low background.[6-10] Among the ECL systems, $Ru(bpy)_3^{2+}$ has received considerable attention due to high ECL efficiency.[11] What's more, solid-state $Ru(bpy)_3^{2+}$ ECL by immobilizing $Ru(bpy)_3^{2+}$ on electrodes surface provides several advantages over solution-phase ECL sensors, for it can reduce consumption of expensive reagents, simplify experimental design and enhance the ECL signal.[12-14] Recently, the appliance of nanoparticles to immobilize $Ru(bpy)_3^{2+}$ has been widespread.[15-21] Graphene, due to the high surface areas, low cost, and high conductivity,[22] holds great promise for potential applications in many technological fields.[23,24] In order to capitalize on the properties of graphene, diverse methods of chemical modification/doping have been developped.[25,26] Accordingly, ECL sensors based on graphene have faster response, better stability and larger ECL intensities.[27,28]

The key to chiral recognition is the fabrication of the chiral interface materials. There are various approaches to construct effective chiral sensing interface.[29] β-cyclodextrin (β-CD), a cyclic oligosaccharide consisting of seven glucose units, has been widely used as chiral selector to construct chiral materials for specific recognition of guest

molecules.[30,31] There are few reports depicting ECL technique in enantioselective detection amnio acids enantiomers or chiral drugs.[32,33] In this work, the composites of $Ru(bpy)_3^{2+}$-gold nanoparticles, graphene and β-cyclodextrin has been prepared to interact with *D*-/*L*-Pro.

Experimental

Reagents and materials

Ruthenium(II)-tris (2,2'-bipyridyl) chloride·$6H_2O$ was purchased from SunaTech Inc (Zhengzhou, China). β-cyclodextrin was gotten from Aladdin. Graphene Oxide was obtained from Nanjing xianfeng nano Co. (Nanjing, China). *D*- and *L*-proline (99 %), gold chloride ($HAuCl_4$), Hydrazine hydrate (Nafion (5 wt%) were bought from J&k· Chemical (Beijing, China). Ammonia (25-28 %), sodium citrate were purchased from Chemical Reagent Co. (Chongqing, China). Graphene oxide (GO) was obtained from Nanjing Xianfeng nano Co. (Nanjing, China). 0.1 M phosphate buffer solution (PBS) at virous pH values were prepared with KH_2PO_4 and Na_2HPO_4 containing 0.1 M KCl. Other chemical reagents were analytical grade and used without further purification. Double distilled water was used in all experiments.

Apparatus

The ECL measurements were carried out with a MPI-A electrochemiluminescence analyzer (Xi'an Remax Analysis Instrument Co., Ltd.) with the voltage of the photomultiplier tube (PMT) set at 800 V. A conventional three-electrode setup containing a modified glassy carbon electrode (GCE, 4.0 mm in diameter) as working electrode, a platinum auxiliary electrode, and a Ag/AgCl (saturated KCl) reference electrode was adopted. Morphologies of the nanomaterials were determined by a scanning electron microscope (SEM, S-4800, Hitachi, Tokyo, Japan). Confocal Laster Raman Spectromet (Kenishaw Trading Co Ltd, Shanghai) was used to carry out the Raman spectroscopy. The FTIR spectrograms were obtained from Fourier Transform Infrared Spectrometer (Perkinelmer, USA).

Preparation of the Ru-AuNPs composites

AuNPs with a diameter of about 12 nm were prepared by sodium citrate reduction of $HAuCl_4$ in aqueous solution.[34] For preparing Ru-AuNPs, 2 mL of 0.5 mg mL^{-1} $Ru(bpy)_3^{2+}$ aqueous solution was added into 5 mL of AuNPs solution under vigorously stirring at room temperature.[35] Several minutes later, large amount of black precipitate was formed. The resulting precipitate was collected by centrifugation and washed with ultrapure water for three times. The obtained Ru-AuNPs composites was redissolved in 1 mL ultrapure water.

Synthesis of the β-CD-rGO nanosheets

The β-CD-rGO nanosheets were synthetized according to the literature.[36] In brief, 5 mL homogeneous graphene oxide dispersion (0.5 mg mL^{-1}), 5 mL of 80 mg mL^{-1} β-cyclodextrin(β-CD) aqueous solution and 75 μL of ammonia solution was mixed completely, followed by the addition of 5 μL of hydrazine solution. And the mixed solution was well-distributed by vigorously stirring for a few minutes at room temperature. Then the vial was put in a water bath (60 °C) for 3.5 h. Stable black dispersion was obtained. The β-CD-rGO nanosheets were collected by centrifugation, and carefully washed with ultrapure water. The obtained nanosheets were redispersed in 5 mL ultrapure water. When not in use, it was stored at 4 °C.

Fabrication of the modified electrodes

Before modification, the glass carbon electrodes (GCE) (Ø = 4 mm) were first polished with 1.0, 0.3, 0.05 μm alumina slurry respectively, followed by rinsing thoroughly with ultrapure water. After that, the electrodes were successively sonicated in ultrapure water, ethanol, ultrapure water separately and dried at the room temperature.

The obtained Ru-AuNPs composites and β-CD-rGO nanosheets and 2.5 wt % Nafion was mixed completely at the aid of sonication (about 0.25 mg mL^{-1} β-CD-rGO) to get the stereoselective ECL nanohybrids (denoted as CGRA). For fabrication of the modified electrodes, 10 μL resulting nanohybrids was dropped onto the glass carbon electrode (GCE) and dried at the room temperature (denoted as CGRA/Nafion/GCE). When not in use, the modified electrodes were stored at 4°C.

Results and discussion

Characteristics

Raman spectroscopy is widely used to study the ordered and disordered crystal structures and scanning-electron-microscope (SEM) to characterize the morphologies and distribution of the nanomaterials, they were used to characterize β-CD-rGO nanosheets, Ru-AuNPs composites, and CGRA nanohybrids. Pristine graphite (Fig. 1A, a) displayed a prominent G band at 1580 cm^{-1}, corresponding to the first-order scattering of the E_{2g} mode observed for sp^2 domains, in addition to a tiny D band at 1352 cm^{-1}, which was ascribed to edge planes and disordered structures.[37] While the graphene oxide (GO) (Fig. 1A, b) showed a broadened and shifted G band to 1595cm^{-1}, and the strongly strengthened D band at 1352 cm^{-1} indicating the shrinking of the in-plane sp^2 domains, which might be due to the extensive oxidation.[38] For β-CD-rGO (Fig. 1A, c), the G band and D band (at 1590 and 1352 cm^{-1}, respectively) were coexisted still, whereas there was a slightly change of the intensity ratio of D/G comparing to GO. This change indicated that the average size of the sp^2 domains decreased after the reduction of GO and that the number of edge planes and the degree of disorder in rGO both increased, indicating

the the creation of numerous new graphitic domains in β-CD-rGO. [36,39]

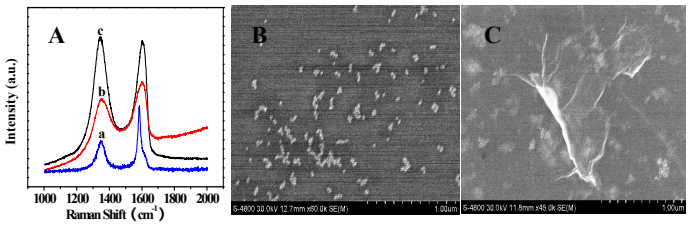

Fig. 1. (A) Raman spectra of graphite (a), GO (b), β-CD-rGO (c); SEM images of the Ru-AuNPs composites (B); CGRA nanohybrids (C).

Fig. 1 B showed the appearance of Ru-AuNPs composites existed in aggregated form, which was attributed to the electrostatic interactions between $Ru(bpy)_3^{2+}$ and negatively charged AuNPs. The SEM image of CGRA nanohybrids was presented in Fig. 1C, the dense coverage of Ru-AuNPs could be observed on the wrinkled β-CD-rGO surface, hinting the high surface areas of rGO may act as an effective matrix to immobilize more Ru-AuNPs.

The discussion of the reaction mechanism

Amino acids could take part in the ECL reactions with $Ru(bpy)_3^{2+}$, which would act as oxidative-reduction co-reactants of $Ru(bpy)_3^{2+}$. Amino acids could take part in the ECL reactions with $Ru(bpy)_3^{2+}$, which would act as oxidative-reduction co-reactants of $Ru(bpy)_3^{2+}$. The ECL mechanism of reaction between $Ru(bpy)_3^{2+}$ and proline has been discussed: at the electrode surface, the immobilized $Ru(bpy)_3^{2+}$ was oxidized to $Ru(bpy)_3^{3+}$ in eq. 1, while the negatively charged proline (pH 8.5, isoelectric point is 6.3) [40,41] was also oxidized to produce free radical in eq. 2.[42,43] As described by eqs 3 and 4, the radical would undergo a deprotonation process to produce an intermediate radical ion, which could react with $Ru(bpy)_3^{3+}$ to produce the excited state $Ru(bpy)_3^{2+*}$ resulting in light emission.[44-46] Following that, the amino group presented in by-product of proline might generate a secondary amine following by a dealkylation process in the presence of water.[45,47-48] The mechanism of $Ru(bpy)_3^{2+}$-proline might be presumably analogous to that of the TPrA–$Ru(bpy)_3^{2+}$ system.[42,49,50] The reaction processes were illustrated as follows:

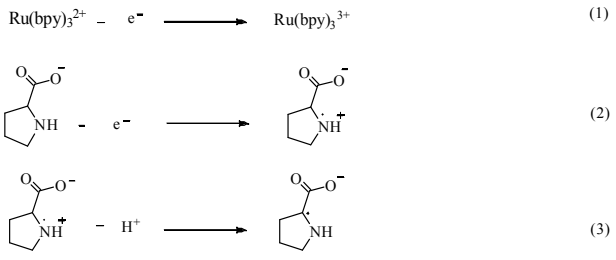

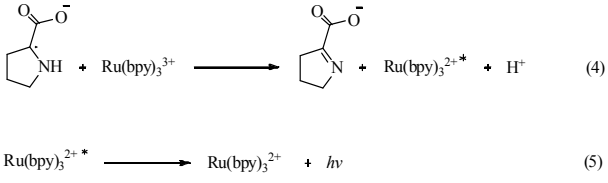

In our work, Pro enantiomers as the analyte participated in the ECL of $Ru(bpy)_3^{2+}$, which would yield more ECL emission. As illustrated in Fig. 2, when Pro absent from the detection solution, obvious decreased ECL intensity of $Ru(bpy)_3^{2+}$ was obtained, which could further confirm the feasibility of ECL sensor based on $Ru(bpy)_3^{2+}$ in the dectection of proline.

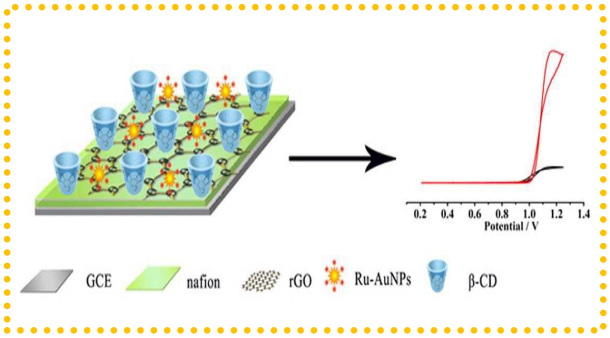

Fig. 2. Reaction scheme of ECL on surface of the proposed sensor.

Enantioselective recognition for Pro enantiomers via ECL

Based on the theories above, the designed electrodes were tested with the potential sweeping from 0.2 V to 1.25 V in 0.1 M phosphate buffer solution (PBS, pH 8.5) containg 5 mM *D*-/*L*- Pro. As shown in Fig. 3A, a great difference was observed on the ECL intensities between the *D*-Pro (curve a) and *L*-Pro(curve b), and the intensity of *D*-Pro was higher than *L*-Pro, which might be caused by the synergistic effects of the nano-materials.

In order to examine ECL performances of the modified electrode without β-CD (denoted as GRA/nafion/GCE), corrresponding measurements have been carried out. Fig. 3B showed that the ECL intensity decreased sharply and the value of difference (ΔI) between *L*-/*D*-Pro was also decreased without β-CD. In our study, β-CD was used as a chiral selector which might play a key role in the different ECL intensities from *D*- or *L*-Pro. It may capture proline inside the cavity to react with $Ru(bpy)_3^{2+}$ on the surface of modified electrode, which could explain the sharp decrease of ECL intensity.[51,52] In addition, it was also a good dispersing reagent for graphene.[53,54] Therefore, the combination of β-CD and rGO could improve the solubility and electrochemical sensing performance comparing to unmodified graphene.[36,39]

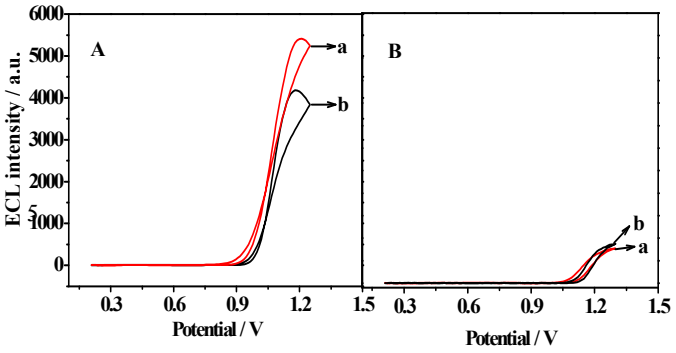

Fig. 3. (A) ECL intensity-potential curves of CGRA/Nafion/GCE in 5 mM *D*-Pro (a) or *L*-Pro (b); (B) ECL intensity-potential curves of GRA/Nafion/GCE in 5 mM *D*-Pro (a) and *L*-Pro (b). 0.1 M PBS (pH 8.5, containing 0.1 M KCl) was used

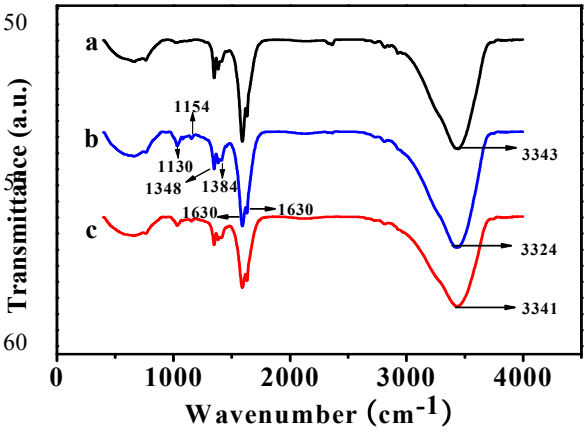

Fig. 4. FT-IR spectra of CGRA (a), *D*-Pro/CGRA (b), and *L*-Pro/CGRA (c).

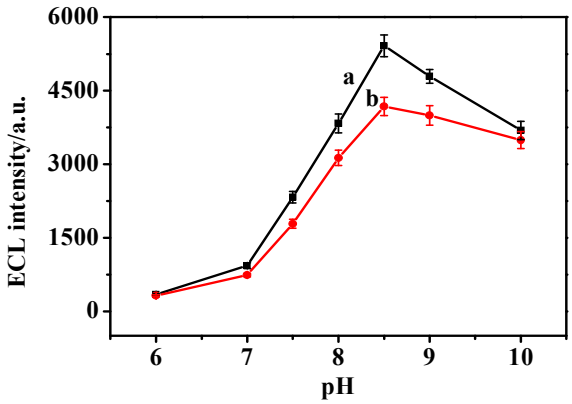

Fig. 5. The effect of pH on the ECL intensities of the CGRA/Nafion/GCE in 5 mM *D*-Pro (a) or *L*-Pro (b).

Mechanism of chiral recognition

The mechanism of enantiomeric selectivity may be due to the combination of different molecular interactions such as H-bonding and dipolar and steric interactions between hydroxyl groups of β-CD and proline.[5,52,55] Hydrogen bonding of polar −(NH)s− of proline to the −(HO)s on β-CD rims would take place when forming the inclusion complex of proline within the hydrophobic central cavity. What's more, the steric interactions between the *D*-/*L*-proline and the chiral carbons of *D*-glucose units of β-CD may also play a role in the chiral recognition.[56] FT-IR spectra was used to investigate the hydrogen bonds between the proline and the proposed chiral interface based β-CD.[57] Based on the results of the FT-IR spectra (shown in Fig. 4), the O-H stretching vibration peaks for CGRA (curve a) and *L*-Pro/CGRA (curve c) appeared at 3343 cm^{-1} and 3341 cm^{-1} respectively, and a slightly red shift peak was located at 3324 cm^{-1} from *D*-Pro/CGRA (curve b).[36,58] From the understanding of the molecular level, the O-H stretching vibration peak could exhibit typical red-shift when hydrogen bonding is formed.[59] The results showed that more hydrogen bonds would be formed between *D*-proline and chiral sensing platform than *L*-proline. In this case, the –NH– in the *L*-enantiomers positioned less favorably for hydrogen bonding, leading to less inclusion complexation with chiral sensing platform, which may explain the chiral recognition.

The influence of pH

The pH of the working buffer is an important influencing factor for the ECL intensities of $Ru(bpy)_3^{2+}$ and the sensitivity of the modified electrodes. Because OH^- takes participate in the reaction of $Ru(bpy)_3^{2+}$ and proline. The influence of the pH values ranging from 5.0 to 10.0 was investigated. As shown in Fig. 5, the highest ECL intensity and optimum chiral discrimination appeared at pH 8.5. Thus, the buffer solution of pH 8.5 was selected for further the experiments.

Application of the enantioselective sensor

Fig. 6 showed the designed sensor was performed in quantitative analysis, for the ECL intensities increased with the increasing concentrations of *L*-Pro or *D*-Pro and displayed a linear with *D*-Pro or *L*-Pro in the range from 1.0×10^{-4} to 5.0×10^{-3} M. The regression equation was $I_{D\text{-}}$=66.86+1056.86c or $I_{L\text{-}}$=73.84+805.46c, and the detection limit was 2.5×10^{-5} M and 3.3×10^{-5} (S/N=3), respectively. Comparing with *L*-Pro, the *D*-Pro obtained a higher ECL intensity with the designed ECL sensor. All of above results demonstrated the proposed stereoselective ECL sensor may provide a new perform on chiral discrimination of Pro enantiomers.

The stability and reproducibility of the sensor

In present work, at the optimum pH 8.5, the investigation of stability of the sensors was carried out by immersing the sensors in 5 mM *D*-/*L*-Pro. After consecutive cyclic potential scans for 11 cycles at a scan rate of 100 mV/s, the intensities of sensor were observed remaining stable (in Fig. 7). The reproducibility of the sensors was examined in 5 mM *D*-Pro

(pH 8.5) by preparing ten electrodes. The ECL intensities of the ten independent electrodes were similar and the relative standard deviation (RSD) was 4.9%, which achieved an acceptable target.

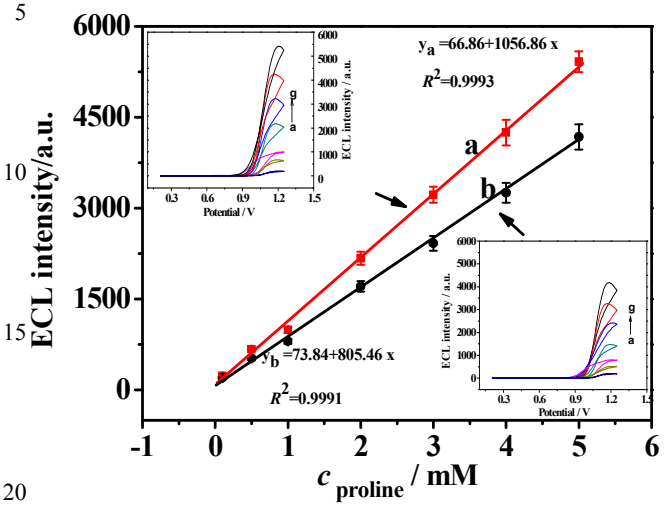

Fig. 6. The calibration plots with increasing concentrations of 0.1, 0.5, 1.0, 2.0, 3.0, 4.0 and 5.0 mM for *D*-Pro (a) and *L*-Pro (b) determination in 0.1 M PBS buffer (pH 8.5) [insets: ECL intensities of *D*-Pro and *L*-Pro with different concentrations, respectively].

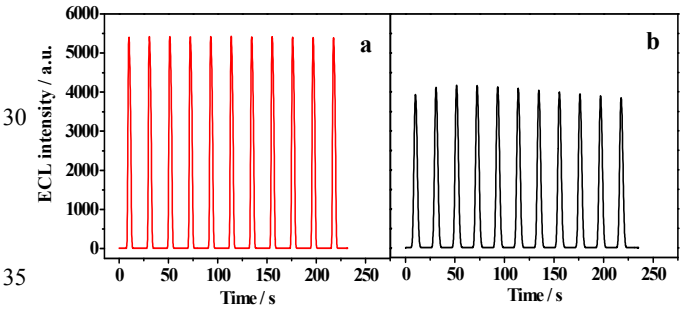

Fig. 7. ECL intensity-time curves of CGRA/Nafion/GCE in PBS (pH 8.5) containing 5 mM *D*-Pro (a) and *L*-Pro (b) under continuous cyclic potential scans for 11 cycles.

The selectivity of the sensor

In order to examine the selectivity of the designed sensor, the experiments for determination of more amino acids with the concentren of 5 mM were carried out. The amino acids used to study the interference were arginine (Arg), phenylalanine (Phe), lysine (Lys), tyrosine (Tyr), histidine (His), valine (Val), alanine (Ala), glutamic acid (Glu), cysteine (Cys) , serine (Ser), tryptophan (Trp) and glutamine (Gln). As shown in Fig. 8, proline exhibited substantially greater chemiluminescence responses than other amino acids. The selectivity observed was due to proline containing the only secondary amine group of the naturally occurring amino acids.[60] For the other primary amino acids, the CL intensity of the reaction of primary amino acids with $Ru(bpy)_3^{3+}$ varies with the electron-withdrawing character of the R-group attached to the α-carbon of the amino acid. Brune and Bobbitt have previously shown that amino acids with poorer electron-withdrawing characteristics could exhibit higher CL intensity.[61] This could be well explained the good selectivity of the proposed sensor towards Pro enantiomers.

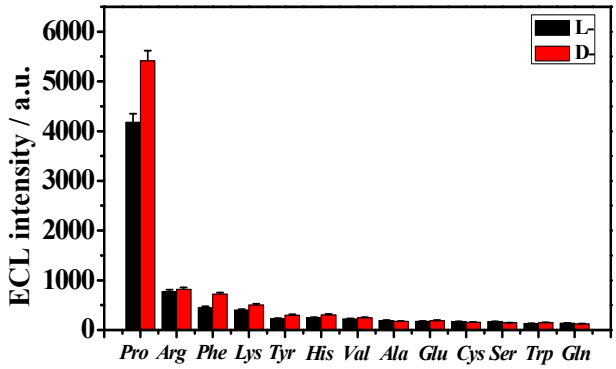

Fig. 8. Comparison of enantioselectivity of 13 kinds of amino acids (5 mM) on the CGRA/Nafion/GCE in PBS (pH 8.5).

Conclusions

In summary, a novel stereoselective ECL sensor was constructed based on β-CD-rGO and Ru-AuNPs, which was applied to discriminate Pro enantiomers. When the *D*-/*L*-Pro involved in the ECL of $Ru(bpy)_3^{2+}$, the ECL response was enhanced greatly. Because of the secondary amine group of proline, it has the better ability of enhancing the ECL emission than the other naturally occurring amino acids containg primary amine group. The results of the experimentsrevealed that the ECL sensor exhibited obviously different ECL intensities towards Pro enantiomers, and a larger ECL intensity was obtained from *D*-Pro. Moreover, the experimental results also indicated that the selectivity, sensitivity, stereoselectivity, stability of the ECL sensor was acceptable. Hence, such an ECL sensor provides a promising method for the detection of amino acids or chiral drugs based on the same principle.

Acknowledgments

The authors gratefully acknowledge financial support for this study by the National Natural Science Foundation of China (No. 21272188).

Notes and references

1 J. Labuta, S. Ishihara, T. Šikorský, Z. Futera, A. Shundo, L. Hanyková, J. V. Burda, K. Ariga1, and J. P. Hill, *Nature communications*, 2013, **4**, 1-8.

2 M. X. Zhang, G. Y. Qing and T. L. Sun, *Chem. Soc. Rev.*, 2012, **41** 1972-1984.

3 R. T. Fremeau, M. G. Caron, R. D. Blakely, *Neuron*, 1992, **8**, 915-926.

4 K. Hamase, S. Takagi, A. Morikawa, R. Konno, A. Niwa . K. Zaitsu, *Anal Bioanal Chem*., 2006, **386**, 705–711.
5 D. Kampel, R. Kupferschmidt and G. Lubec, *Amino Acids*, 1990 1164-1171.
6 P. Bertoncello, R. J. Forster, *Biosens. Bioelectron*., 2009, **24**, 3191- 3200.
7 A. J. Bard, Electrogenerated Chemiluminescence. New York: Marcel Dekker, 2004.
8 W. J. Miao, *Chem. Rev*., 2008, **108**, 2506–2553.
9 M. M. Richte, *Chem. Rev*., 2004, **104**, 3003−3036.
10 Z .Y. Liu, W.J. Qi and G.B. Xu, *Chem. Soc. Rev.*, 2015, **44**, 311.
11 B. A. Gorman, P. S. Francis and N. W. Barnett, *Analyst*, 2006, **131**, 616–639.
12 L. H. Zhang, X. P. Sun, and S. J. Dong, *Biosens. Bioelectron*., 2007, **22**, 1097–1100.
13 L. L. Li, K. Liu, G. H. Yang , C. M. Wang , J. R. Zhang ,and J. J. Zhu, *Adv. Funct. Mater.* 2011, **21**, 869–878.
14 Z. H. Guo, Y. Shen, M. K. Wang, F. Zhao, and S. J. Dong, *Anal. Chem.*, 2004, **76**, 184–191.
15 Y. He, Y. Q. Chai, R. Yuan, *Biosens. Bioelectron.*, 2013, **50**, 294–299.
16 E. Rampazzo, S. Bonacchi, D. Genovese, R. Juris, M. Marcaccio, M. Montalti, F. Paolucci, M. Sgarzi, G. Valenti, N. Zaccheroni and L. Prodi, *Coord. Chem. Rev*., 2012, **256**, 1664–1681.
17 G. Valenti, E. Rampazzo, S. Bonacchi, T. Khajvand, R. Juris, M. Montalti, M. Marcaccio, F. Paolucci and L. Prodi, *Chem. Commun.*, 2012, **48**, 4187–4189.
18 K. Kadimisetty, S. Malla, N. P. Sardesai, A.A. Joshi, R. C. Faria, N. H. Lee, and J. F. Rusling, *Anal. Chem*., 2015, **87**, 4472−4478.
19 D. F. Wang, L. H. Guo, R. Huang, B. Qiu, Z. Y. Lin and G. N. Chen, *Scientific Reports*, 2015, **5**, 7954.
20 X. P. Sun, Y. Du, S. J. Dong, E. K .Wang, *Anal. Chem*., 2005, **77**, 8166 -8169.
21 G. F. Gui, Y. Zhuo, Y. Q. Chai, N. Liao, M. Zhao, J. Han, Y. Xiang and R. Yuan, *RSC Adv*.**,** 2014, **4**, 1955-1960.
22 A. K. Geim, K. S. Novoselov, *Nature Materials*. 6 (2007) 183-191.
23 A. K. Geim, *Science* 2009, **324**, 1530-1534.
24 B. Seger, P. V. Kamat, *Phys. Chem. C.*, 2009, **113**, 7990–7995.
25 U. N. Maiti , W. J. Lee, J. M. Lee, Y. Oh , J. Y. Kim , J. E. Kim ,J. Shim , T. H. Han , and S. O. Kim , *Adv. Mater.*, 2014, **26**, 40–67.
26 S. Bai and X. P Shen，*RSC Adv.*, 2012, **2**, 64-98.
27 Y. Y. Su and Y. Lv, *RSC Adv*.**,** 2014, **4**, 29324-29339.
28 W. H. Gao, Y. S. Chen, J. Xi, A. Zhang, Y. W. Chen, F. S. Lu, Z. G. Chen, *Sensors and Actuators B: Chemical*, 2012, **171**, 1159-1165.
29 K. Ariga, Y. Yamauchi, G. Rydzek, Q. Min Ji, Y. Yonamine, K. C.-W. Wu, and J. P. Hill, *Chem. Lett*., 2014, **43**, 36–68.
30 D. W. Armstrong, T. J. Ward, R. D. Armstrong, and T. E. Beesley, *Science*, 1986, **232**, 1132-1135.
31 J. Zhou,Y. Dai, S. Y Wang, E. W Zhu, J. F Hai, Y. Liu, J. Tang and W. H Tang, *RSC Adv*.**,** 2012, **2**, 5088-5093.
32 C. Z. Zhao, S. Y. Xu, Y. Su and G. L. Zhao, *Analyst*, 2002, **127**, 889–891.
33 L. Wu, C. Q. Zhao, J. S. Ren, and X. G. Qu, *Chem. Eur. J.*, 2014, **20**, 11675–11679.
34 G. Frens, *Nat. Phys. Sci.* 1973, **241**, 20.
35 M. Li, M. Zhang, S. G. Ge, M. Yan, and J. H. Yu, *Sensors and Actuators B: Chemical*, 2013, **181**, 50–56.
36 Y. J. Guo, S. J. Guo, J. T. Ren, Y. M. Zhai, S. J. Dong, and E. K Wang, *ACS. Nano*., 2010, **4**, 4001-4010.
37 M. S. Dresselhaus, A. Jorio, M. Hofmann, G. Dresselhaus, and R. Saito, *Nano Lett*., 2010, **10**, 751–758.
38 Y. W. Zhu, S. Murali, W. W. Cai, X. S. Li, J. W. Suk, J. R. Potts, and R. S. Ruoff, *Adv. Mater*., 2010, **22**, 3906–3924.
39 L. Tan, K. G. Zhou, and Y. H. Zhang, *Electrochemistry Communications*., 2010, **12**, 557-560.
40 L. Pogliani, *Journal of Pharmaceutical Sciences*, 1992, **81**, 334-336.
41 S.Yamada, C. Hongo, and I. Chibata, *Agricultural and Biological Chemistry*, 1977, **41**, 2413-2416.
42 M. Hosseini, M. R. Moghaddam, F. Faridbod, P. Norouzi, M. R. K. Purb and M. R. Ganjali, *RSC Adv.,* 2015, **5**, 64669.
43 Y. F. Zhuang, H. X. Ju, *Electroanalysis*, 2004, **16**, 1401-1405.
44 H. Hosono, W. Satoh and H. Suzuki, *Sensors and Materials*., 2007, **19**, 191-201.
45 R. J. Forster, C. F. Hogan, *Anal. Chem.* 2000, **72**, 5576-5582.
46 J. G. Li, Q. Y. Yan, Y. L. Gao, and H. X. Ju, *Anal. Chem.* 2006, **78**, 2694-2699.
47 X. Chen , C. Q. Yi , M. J. Li , X. Lu , Z. Li , P. W. Li , X. R. Wang, *Analytica Chimica Acta.*, 2002, **466**, 79–86.
48 A. W. Knight, G. M. Greenway, *Analyst*, 1996, **121**, 101R-106R.
49 H. W. Sun, M. Su, and L. Q. Li, *Journal of Chromatographic Science*, 2010, **48**, 49-54.
50 W. J. Miao, *Chem. Rev.* 2008, **108***,* 2506–2553.
51 H. Dai, C. P. Yang, X. L. Ma, Y. Y. Lin and G. N. Chen, *Chem. Commun*., 2011, **47**, 11915-11917.
52 L. Szente and J. Szeman, *Anal. Chem*. 2013, 85, 8024−8030.
53 K. S. Liu, H. G. Fu, Y. Xie, L. L. Zhang, K. Pan, and W. Zhou, *J. Phys. Chem. C*., 2008, **112**, 951-957.
54 B. Konkena and S. Vasudevan, *Langmuir* 2012, **28**, 12432−12437.
55 Y. X. Tao, .J. Y. Dai, Y. Kong, and Y. Sha, *Anal. Chem*. 2014, **86**, 2633−2639.
56 D. W. Armstrong, T. Ward, R. D. Armstrong, T. Beesley, *Science*, 1986, **232**, 1132−1135.
57 .X. Zhang, J. Yin, and J. Yoona, *Chem. Rev*., 2014, **114**, 4918−495.
58 M. Yoshida, Y. Hatate, K. Uezu, M. Goto, S. Furusaki, *Colloids and Surfaces A: Physicochemical and Engineering Aspects*, 2000, **169**, 259–269.
59 L. F. Scatena, M. G Brown, and G. L Richmond, *Science,* 2001, **292**, 908–912.
60 W. Jackson, D. R. Bobbitt, *Anal. Chim. Acta*, 1994, **285**, 309–320.
61 S. N. Brune and D. R. Bobbitt, A*nal. Chem*. 1992, **64**, 166.